

This article has been published in Materials Letters. The final publication is available from Elsevier at <https://doi.org/10.1016/j.matlet.2020.128057>.

Composite Dip Coating Improves Biocompatibility of Porous Metallic Scaffolds

Joseph Deering¹, Amanda Clifford¹, Andrew D'Elia¹, Igor Zhitomirsky^{1,2}, Kathryn Grandfield^{1,2*}

¹ Department of Materials Science and Engineering, McMaster University, Hamilton, ON, Canada

² School of Biomedical Engineering, McMaster University, Hamilton, ON, Canada

* Corresponding author:

Prof. Kathryn Grandfield
McMaster University
1280 Main Street West
Hamilton, ON, L8S 4L7
Canada
Email: kgrandfield@mcmaster.ca

Abstract

Porous materials are becoming more common for bone implants, and it is increasingly important to find surface modification strategies that affect both the implant exterior and porous interior. In this study, selective laser melting (SLM) was used to create porous stainless steel implants 8 mm in diameter, which were subsequently dip coated with a composite polymethylmethacrylate-alumina (PMMA- Al_2O_3) film. Imaging with electron microscopy found evidence of the films at a depth of 2.2 mm into the porous implants, with dual-scale topography created by the native SLM stainless steel substrate and alumina nanoparticles. Energy dispersive X-ray spectroscopy confirmed the presence of the coating along the periphery of interior pores. *In vitro* tests with osteoblast-like cells showed greater cell metabolism on composite-coated samples compared to uncoated dense samples after seven days of culture.

Keywords

Dip coating, polymethylmethacrylate, additive manufacturing, porous materials, osseointegration, sol-gel preparation

1 Introduction

Porous metallic implant materials are becoming increasingly common for usage in bone and joint replacement due to their ability to mitigate stress-shielding effects[1]. The use of additive manufacturing enables effective scaffold design in bone implants by creating tunable mechanical performance[2] and channels for mass transport[3] by implementing porosity.

To encourage bone ingrowth, implants have been coated with composite materials, which can contain bioceramic particles such as calcium phosphate[4], rutile[5], and alumina[6]. One key limitation of conventional coating techniques, such as plasma spraying, is their line-of-sight processing[7], which prevents uniform coating deposition in the interior of porous structures, and their high-temperature processing. Changing the surface composition and topography in the interior of porous specimens is possible by electrochemical methods, such as micro-arc oxidation[8,9], where oxides of the base metal, calcium, or phosphorus are added to the surface. Composite materials have also been developed as a feedstock for additive manufacturing processes as a means of modifying the interior of porous structures compared to structures produced by traditional titanium feedstocks[10]. Recently, immersion techniques[11] and electrophoretic deposition[12] have been effective for depositing bioactive and organic coating materials on the interior of porous structures. Where alumina-based ceramic materials have been traditionally used for bulk implant components due to their excellent biocompatibility in bone applications[13], their integration in nanoparticle form on the interior of porous constructs has not been evaluated. Polymethylmethacrylate (PMMA), commonly known as a primary constituent in some bone cements, has recently been shown to have favourable osteogenic effects as an implant coating[14]. The potential for PMMA-Al₂O₃ organic composite material to coat the interior of porous metallic scaffolds remains unexplored.

The objective of this work was the development of a facile dip coating method to deposit a composite PMMA-alumina coating on the interior of an additively manufactured porous scaffold. Scanning electron microscopy (SEM) was used to confirm deposition, and the potential for improving osseointegration was explored with an *in vitro* cell metabolism assay.

2 Methods

2.1 Scaffold Production

Cylinders ($h = 8$ mm, $\phi = 8$ mm) were designed in Autodesk Netfabb and hollowed to create body-centred cubic lattice struts rotated 45° about the X and Y axes. Fully dense implants as well as porous implants with strut diameters of 450 μm with a unit cell spacing of 1.2 mm, and therefore pores with an approximate throat diameter of 275 μm were formed. Scaffolds were built using 304L stainless-steel powder (< 45 μm , Carpenter Additive) using the selective laser melting (SLM) process (EOSINT M280, Germany). Laser power was set to 200 W, scan speed 800 mm/s, hatch spacing 80 μm , and layer thickness 40 μm during fabrication. Metal scaffolds were cleaned with ethanol and deionized water in an ultrasonic bath for 20 min. Scaffolds were either kept whole or sectioned longitudinally for subsequent coating.

2.2 Coating Deposition and Characterization

Polymethylmethacrylate (MW ~ 120,000, Millipore Sigma) and alumina (0.13 μ m, Al₂O₃, Baikowski) particles were obtained. Under continuous stirring, 10 g L⁻¹ PMMA was added to a mixed solvent containing 20% deionized water and 80% isopropanol (Millipore Sigma) and heated to 55°C, at which point the PMMA fully dissolved, only marginally increasing the viscosity. The PMMA solution was cooled back to room temperature, and Al₂O₃ particles were added to a concentration of 10 g L⁻¹. Metallic scaffolds were coated whole to produce specimens for cell viability assays or in halves for easier investigation of the midplane with electron microscopy. Scaffolds were attached to copper tape (see Figure S1), immersed into the PMMA-Al₂O₃ suspension under sonication for one minute, removed, and air dried at room temperature for 24 hours to evaporate solvent.

The mid-plane of the scaffold was sputter coated with carbon for conductivity, mounted to a SEM stub with silver paint and analyzed by SEM imaging (FEI Magellan 400) and energy dispersive X-ray spectroscopy (EDS) using an accelerating voltage of 10 kV.

2.3 Cell Viability

Saos-2 osteosarcoma cells (ATCC) were seeded on additively manufactured solid implants, porous implants, and PMMA-Al₂O₃ coated porous implants at a density of 10,000 cells/cm² in McCoy's Modified 5A media. Cells were cultured at 37°C in an atmosphere of 5% CO₂ for seven days. After one, three, and seven days, a solution of 5% alamarBlue reagent in media (Life Technologies Inc.) was added to wells for 60 min. The dye was pipetted into a separate plate and fluorescence was measured at an excitation-emission wavelength of 540-580 nm. Statistical significance was determined using a two-way ANOVA in R with Tukey's HSD test and $p < 0.05$.

3 Results and Discussion

3.1 Coating Deposition

Dip coating with the PMMA-Al₂O₃ composite produced a coating on both the exterior and interior of the scaffolds. Where PMMA bonds to the substrate may be governed by bidentate ligands, the mechanical strength of the composite coating on the stainless steel substrate is possibly increased compared to other coatings with monodentate bonding coordination. Higher magnification images of a representative pore (Figure 1A) illustrate the presence of the composite coating at an interior site, where non-uniform thickness is observed around the periphery of the pore. There is also evidence of sintered stainless steel particles on the lattice struts within the pores, adding elements of microscale topography on both interior and exterior lattice sites. Nanoparticles of Al₂O₃ were observed to be uniformly distributed through the PMMA matrix without aggregation (Figure 1B) at interior sites of the scaffolds. These nanoparticles, in conjunction with inherent striations in the PMMA matrix, add elements of nanoscale topography to interior and exterior sites in the scaffold, which can be favourable for osseointegration[15]. Coating deposition on the interior appears consistent with the exterior (Figure 1C), where Al₂O₃ is evenly distributed through the PMMA.

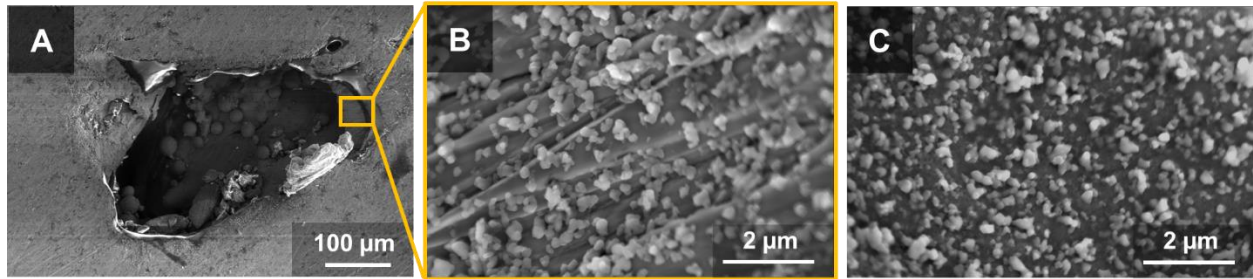


Figure 1: (A) Image of a representative pore on the interior of the scaffold. Thickness of PMMA- Al_2O_3 around the pore periphery is not constant. (B) Surface topography of PMMA- Al_2O_3 composite coating at the scaffold interior. (C) Surface topography of the PMMA- Al_2O_3 composite coating at the scaffold exterior. The Al_2O_3 distribution is comparable at scaffold exterior and interior sites.

EDS maps at interior scaffold sites (Figure 2A) on the cross-section are shown in Figure 2B, 2C, and 2D. Each site has a different distance to the scaffold exterior. Elemental signals characteristic to the uncoated stainless-steel (Fe, Ni) were uniform on the cross-sectional surface, while signals characteristic to the composite coating (C, Al) displayed higher intensity directly around the pore periphery at depths of 0.4 mm, 1.2 mm, and 2.2 mm.

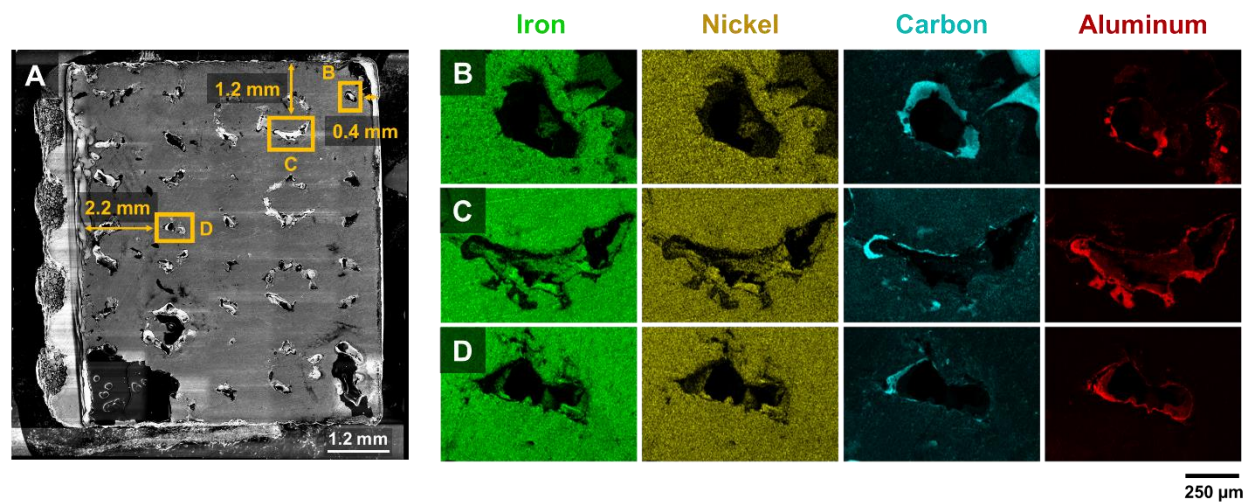


Figure 2: (A) Cross-sectional SEM image with bright regions representative of the coating. Sampling sites at various distances to exterior correspond to EDS maps at depths of 0.4 mm (Row B), 1.2 mm (Row C) and 2.2 mm (row D). Increased intensity of aluminum and carbon at the pore periphery indicates complete penetration of the coating into the interior pores.

3.2 Cell Viability

The results of cell viability assays on the solid implants, porous implants, and PMMA- Al_2O_3 coated porous implants are shown in Figure 3. After seven days of culture, the PMMA- Al_2O_3 coated scaffolds significantly outperformed dense stainless-steel samples, confirming what has been shown previously on two-dimensional substrates[14]. Statistically higher cell metabolism

was also observed from day one to day seven on both the porous implants without coating and PMMA-Al₂O₃ coated porous implants. These results suggest that the addition of an interconnected porosity network with a diameter of 275 μm allows for rapid cellular proliferation through the porous interior of the scaffold relative to the control. The addition of PMMA-Al₂O₃ composite coatings on porous scaffolds further improves osseointegration potential relative to uncoated implants. By coating the SLM implant surface, surface topography, chemistry, and wettability are modified, and it is probable that metallic particle release is impeded. All of these factors can change the dynamics of cell-surface interaction, contributing to the resulting increase in cell viability seen here.

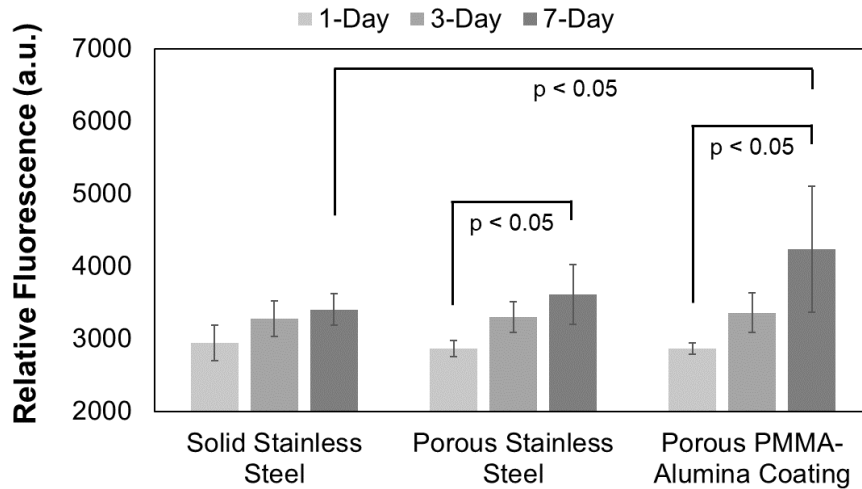


Figure 3: Saos-2 cell viability on solid, porous, and coated porous AM parts. Porous implants coated with the PMMA-Al₂O₃ composite coating showed significantly higher cell proliferation after seven days compared to solid components, while all porous implants showed significantly more cell proliferation after seven days.

4 Conclusions

PMMA-Al₂O₃ composite films were successfully deposited on the porous interior of SLM stainless steel implants using a facile dip coating method. SEM and EDS maps confirmed that the coating penetrated at least 2.2 mm into the scaffold interior, indicating that this immersion technique is suitable for coating the complete interior of porous metallic implants with a biomedical composite material. The alumina nanoparticles also contributed to a nanoscale topography around the pore periphery. *In vitro* characterization of the coated scaffolds with Saos-2 cells showed statistically higher rates of cell metabolism when compared to fully dense structures with the same geometry. Therefore, the dip coating method is a promising approach for creating composite coatings on porous implants to improve the potential osteoconductivity of their interior pores. The successful demonstration of Al₂O₃ nanoparticles, PMMA, and stainless steel scaffolds as pilot materials should lead to investigation of other additives and substrates, such as titanium

alloys, for polymer-composite coatings on porous SLM implants. Future work should also evaluate the limits of PMMA-Al₂O₃ integration in larger-sized implants.

5 Acknowledgements

The authors acknowledge the support of the Natural Sciences and Engineering Research Council of Canada (RGPIN-2014-06-053).

6 References

1. Arabnejad S, Johnston B, Tanzer M, Pasini D. Fully porous 3D printed titanium femoral stem to reduce stress-shielding following total hip arthroplasty. *J Orthopaed Res*. 2017;35(8):1774–83.
2. Wang X, Xu S, Zhou S, Xu W, Leary M, Choong P, et al. Topological design and additive manufacturing of porous metals for bone scaffolds and orthopaedic implants: A review. *Biomaterials*. 2016;83:127–41.
3. Zadpoor AA. Additively manufactured porous metallic biomaterials. *J Mater Chem B*. 2019;7(26):4088–117.
4. Eliaz N, Metoki N. Calcium Phosphate Bioceramics: A Review of Their History, Structure, Properties, Coating Technologies and Biomedical Applications. *Materials*. 2017;10(4):334.
5. Clifford A, Lee BEJ, Grandfield K, Zhitomirsky I. Biomimetic modification of poly-l-lysine and electrodeposition of nanocomposite coatings for orthopaedic applications. *Colloids Surfaces B Biointerfaces*. 2018;176(Polym. (United Kingdom). 121 2017):115–21.
6. McManus AJ, Doremus RH, Siegel RW, Bizios R. Evaluation of cytocompatibility and bending modulus of nanoceramic/polymer composites. *J Biomed Mater Res A*. 2005;72A(1):98–106.
7. Munting E. The contributions and limitations of hydroxyapatite coatings to implant fixation. *Int Orthop*. 1996;20(1):1–6.
8. Xiu P, Jia Z, Lv J, Yin C, Cheng Y, Zhang K, et al. Tailored Surface Treatment of 3D Printed Porous Ti6Al4V by Microarc Oxidation for Enhanced Osseointegration via Optimized Bone In-Growth Patterns and Interlocked Bone/Implant Interface. *ACS Appl Mater Inter*. 2016;8(28):17964–75.
9. Chen Z, Yan X, Chang Y, Xie S, Ma W, Zhao G, et al. Effect of polarization voltage on the surface componentization and biocompatibility of micro-arc oxidation modified selective laser melted Ti6Al4V. *Mater Res Express*. 2019;6(8):086425.
10. Attar H, Ehtemam-Haghighi S, Soro N, Kent D, Dargusch MS. Additive manufacturing of low-cost porous titanium-based composites for biomedical applications: Advantages, challenges and opinion for future development. *J Alloy Compd*. 2020;827:154263.

11. Domínguez-Trujillo C, Peón E, Chicardi E, Pérez H, Rodríguez-Ortiz JA, Pavón JJ, et al. Sol-gel deposition of hydroxyapatite coatings on porous titanium for biomedical applications. *Surf Coatings Technology*. 2018;333:158–62.
12. Kollath VO, Chen Q, Mullens S, Luyten J, Traina K, Boccaccini AR, et al. Electrophoretic deposition of hydroxyapatite and hydroxyapatite–alginate on rapid prototyped 3D Ti6Al4V scaffolds. *J Mater Sci*. 2016;51(5):2338–46.
13. Zeng P. Biocompatible alumina ceramic for total hip replacements. *Mater Sci Tech Ser*. 2013;24(5):505–16.
14. D’Elia A, Deering J, Clifford A, Lee BEJ, Grandfield K, Zhitomirsky I. Electrophoretic deposition of polymethylmethacrylate and composites for biomedical applications. *Colloids Surfaces B Biointerfaces*. 2019;188:110763.
15. Omar O, Karazisis D, Ballo A, Petronis S, Agheli H, Emanuelsson L, et al. The role of well-defined nanotopography of titanium implants on osseointegration: cellular and molecular events in vivo. *Int J Nanomed*. 2016;Volume 11:1367–82.

Composite dip coating improves biocompatibility of porous metallic scaffolds

Joseph Deering^a, Amanda Clifford^a, Andrew D'Elia^a, Igor Zhitomirsky^{a,b}, Kathryn Grandfield^{a,b,*}

^a Department of Materials Science and Engineering, McMaster University, Hamilton, ON, Canada

^b School of Biomedical Engineering, McMaster University, Hamilton, ON, Canada

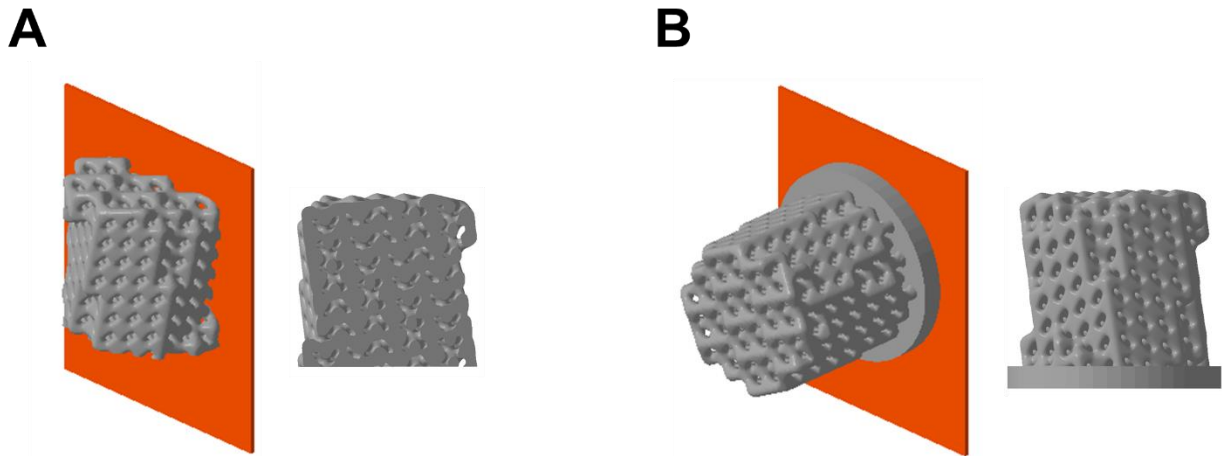


Figure S1: Metallic scaffolds (grey) were either (A) Sectioned longitudinally and mounted along their mid-plane to copper tape (red), or (B) Mounted whole by their baseplate, prior to dip coating in the PMMA- Al_2O_3 suspension.